Int. J. Electrochem. Sci., 12 **(2017)** 7754 – 7764, doi: 10.20964/2017.08.08

International Journal of ELECTROCHEMICAL SCIENCE
www.electrochemsci.org

A Sensor for Detection of 4-nitrophenol Based on a Glassy Carbon Electrode Modified with a Reduced Graphene Oxide/Fe_30_4 Nanoparticle Composite

Yongqiang Cheng, Yaohua Li, Dan Li, Bo Zhang, Runfang Hao, and Shengbo Sang[*]

MicroNano System Research Center, Key Lab of Advanced Transducers and Intelligent Control System of the Ministry of Education & College of Information Engineering, Taiyuan University of Technology, Taiyuan 030024, China
[*]E-mail: sangshengbo@tyut.edu.cn

Received: 12 April 2017 / *Accepted:* 25 May 2017 / *Published:* 12 July 2017

A simple sensor, based on a glassy carbon electrode (GCE) modified with a reduced graphene oxide (RGO) and Fe_3O_4 nanoparticle composites (Fe_3O_4NPs), was developed for detection of 4-nitrophenol (4-NP). The surface morphology of the prepared reduced graphene oxide/Fe_3O_4 nanoparticle composites was characterized by scanning electron microscopy (SEM). The RGO/Fe_3O_4NPs modified GCE was confirmed by cyclic voltammogram (CV) and electrochemical impedance spectroscopy (EIS). The electrochemical behaviors of the as-obtained RGO/Fe_3O_4NPs toward 4-NP were investigated with differential pulse voltammetry (DPV) and square wave voltammetry (SWV). Under the optimal experimental conditions, the linear relationship between the peak current and the concentration of 4-NP was obtained from DPV in the range from 0.2 to 10 μM, 20 to 100 μM and SWV in the range from 0.2 to 10 μM. And respectively, the limit of detection (LOD) of 4-NP was 0.26 μM and 0.86 μM for DPV and SWV. The sensor was used to determine the level of 4-NP in tap water samples with good recovery, highlighting the sensor's feasibility for industrial applications. The proposed sensor provided an efficient performances and acceptable stability for the detection of 4-NP in the water.

Keywords: DPV, electrochemical detection, Fe_3O_4, RGO,4-NP

1. INTRODUCTION

Phenol compounds are widely applied in industry and are used as intermediates in the synthesis of drugs, dyestuffs, various pesticides [1]. The class of phenol compounds has played a considerable role in agriculture because of their high insecticidal activity, but they can cause irreversible damage to organisms and plants even at very low concentration [2,3]. Among them, 4-Nitrophenol (4-NP) is a

breakdown product as well as a chemical intermediate in the production of organophosphorus insecticide derivatives of parathion. So 4-NP is one of the venenous pollutions by the US Environmental Protection Agency. Therefore, it is of great importance to develop methods for the determination of 4-NP in terms of environmental protection and food security.

During the last few decades, several analytical and spectroscopic techniques, such as gas and liquid chromatography [4,5], UV-vis spectrophotometry [6], fluorescence [7], capillary zone electrophoresis[8] and their combined use [9,10], have been proposed for the determination of 4-NP. However, to implement these methods, expensive apparatus and long analysis time are needed. Electrochemical method has drawn considerable attention because of its simplicity, high sensitivity and fast analysis, easy operation, capability of on-line monitoring and low cost. Recently, people began to employ the electrochemical detection method to detect a variety of materials, such as heavy metal ions [11], organophosphorus pesticide [12], DNA hybridization [13], glucose [14] and so on.

Recently, graphene, a new two-dimensional structure consisting of sp^2-hybridized carbon, attracted considerable attention from researchers because of its excellent charge transport mobility, good chemical stability, special π-π conjugate planar geometric structure, high specific surface area (theoretical specific surface area of 2630 m^2/g) and small dimension, great mechanical strength and so on [15,16]. So the extraordinary properties of graphene motivate the development of methods for their use in producing continuous, strong, tough fibres [17,18], new energy batteries [19], flexible screens [20], supercapacitors [21] and sensors [22].

On the other hand, the extensive research work has been done related to magnetite (Fe_3O_4) nanoparticles due to their special attributes, such as low cost, magnetic properties, low toxicity, optical properties, biocompatibility, easy preparation and environmental friendly [23,24]. Now magnetite (Fe_3O_4) can be used for lithium ion batteries [23,25,26], catalyst support [27] medicine [28], electrode material [29] and so on.

So far, RGO/Fe_3O_4NPs has been reported for electrochemical detection method. For example, M.R. Mahmoudian and his team adopted the Fe_3O_4/RGO NSCs/GCE to detect the lead (II) [30], Fangjian Ning and his coworkers adopted MIPs/GO/Fe_3O_4 to extract 17β-Estradiol [31], Najmeh Nazari and his cooperators developed GO/Fe_3O_4 for simultaneous extraction, preconcentration of acidic, basic, and neutral compounds [32], G. Jenita Rani and his team adopted RGO/Fe_3O_4 for detection dopamine [33]. But RGO/Fe_3O_4 have not been used for the detection of 4-NP. Hence, to take the advantages of graphene and Fe_3O_4, we prepared a reduced graphene oxide (RGO) and Fe_3O_4 composites to modify the GCE. These hybrids not only enhance the dispersion stability of Fe_3O_4, but also can prevent the aggregation and restacking of graphene sheets and retain their large surface area due to the presence of Fe_3O_4 nanoparticles [34,35].

2. EXPERIMENTAL

2.1. Reagents

Graphite powder of about 50 μm was purchased from Shanghai Carbon Co., Ltd. 4-NP, HNO_3, anhydrous alcohol, NaH_2PO_4, H_2SO_4, alumina (0.3 and 0.05 μm), Na_2HPO_4, $FeCl_3$, $FeCl_2$, KCl,

$K_4[Fe(CN)_6]\cdot 3H_2O$, $K_3[Fe(CN)_6]$, and H_2O_2 (30 wt %) were purchased from Sinopharm Chemical Reagent C/o., Ltd. (Shanghai, China). All the solutions were prepared using double-distilled water. The 0.067 M phosphate buffer solution (PBS, pH=6.0) was prepared with the addition of solid NaH_2PO_4, Na_2HPO_4. Then add 4-NP to the PBS and sonicate the mixture solution for sufficient dissolution to obtain the 4-NP solution. The 0.01M $[Fe(CN)_6]^{3-/4-}$ was prepared with the $K_4[Fe(CN)_6]\cdot 3H_2O$, $K_3[Fe(CN)_6]$ and KCl.

2.2. Apparatus

All the electrochemical experiments were performed on a ZAHNER-PP211 Electrochemical Workstation from Germany. A conventional three-electrode system was composed of a glassy carbon electrode (GCE) as the working electrode, a Pt foil as the counter electrode, and Ag/AgCl (3 M KCl saturated with AgCl) as the reference electrode, respectively. Cyclic voltammogram (CV), electrochemical impedance spectroscopy (EIS), differential pulse voltammetry (DPV) and square wave voltammetry (SWV) were performed on the ZAHNER-PP211 Electrochemical Workstation. Surface morphology and nanometric structure of samples were obtained by field-emission scanning electron microscopy (FESEM, Hitachi S-4700).

2.3. Preparation of RGO/Fe_3O_4NPs

Graphene oxide (GO) was prepared by a modified Hummers' method [36]. The following steps in [34] are taken to gain the RGO/Fe_3O_4NPs composite. Firstly an aqueous solution of $FeCl_3$ and $FeCl_2$ was prepared with a 2:1 mol ratio. Then mix GO particles with 450 mL of water and stir well. The precursor was prepared by adding iron ions solution into the GO solution at room temperature slowly and adjusted the pH to 10 with 30% ammonia solution (GO = 0.700 g/450 mL, $FeCl_3$ = 3.2442 g/25 mL and $FeCl_2$ = 1.2675 g/25 mL). 10 mL of hydrazine hydrate were added to prepared solution after the temperature of the solution was raised to 90 ℃, then constant stirring, resulting in a black colored solution. After being rapidly stirred for 4 h, the solution was cooled down to room temperature, filtered, washed using water and ethanol several times, and finally dried in vacuum at 70 ℃.

2.4. Preparation of the Modified Electrodes

Bare GCE was successively polished with 0.3 and 0.05 μm of alumina slurry prior to modification. Then, the polished-GCE was sonicated with 1:1 (V/V) HNO_3, anhydrous alcohol and double-distilled water sequentially. The RGO/Fe_3O_4NPs/GCE was obtained by casting 4 μL of this suspension on the surface of a freshly polished GCE and dried at room temperature. Hence, the electrode was modified as RGO/Fe_3O_4NPs/GCE. In order to facilitate comparison, the RGO/GCE was also prepared with the RGO homogeneous suspension in the same procedure described above.

3. RESULTS AND DISCUSSION

3.1. Structural and Surface Properties of RGO/Fe_3O_4NPs

Fig. 1.A presents the typical SEM image of the prepared RGO, and it has a crumpled and rippled sheet structure, and this structure could highly improve the available contact area. The SEM image of the prepared RGO/Fe_3O_4NPs in Fig. 1.B shows the Fe_3O_4NPs with an average diameter of about 50 nm in diameter agglomerate on the RGO supports, suggesting that the Fe_3O_4NPs are successfully adhered to the surface and the inside of RGO and they are well dispersed with little coagulation. And RGO/Fe_3O_4NPs exhibit a significantly irregular surface because of the deposition on RGO.

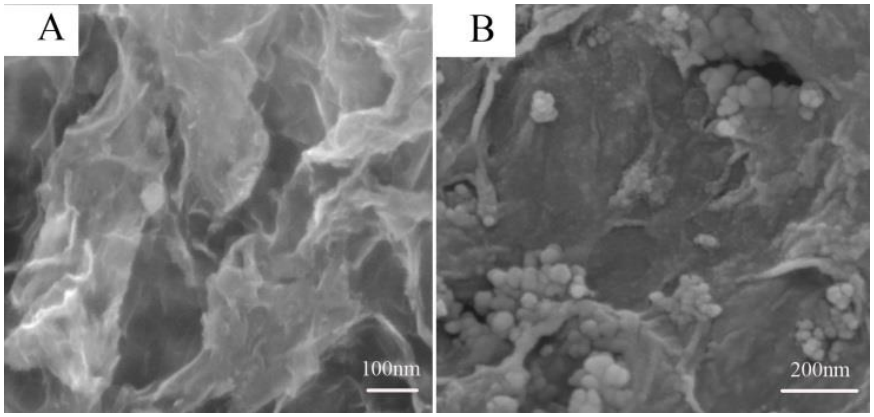

Figure 1. (A) SEM image of the as-prepared RGO, (B) SEM image of the as-prepared RGO/Fe3O4NPs.

3.2. Characterization of Modified Electrodes

Fig. 2 shows the typical cyclic voltammetry (CV) and electrochemical impedance spectroscopy (EIS) of bare GCE and modified GCE in the 0.1 M KCl solution containing 0.01 M $[Fe(CN)_6]^{3-/4-}$, which is sensitive to the surface chemistry of carbon-based electrodes. The Fig. 2.A shows the reduction and oxidation peak current decreased obviously after the modified GCE, and the redox peaks current of RGO/Fe_3O_4/GCE became even lower than the redox peaks current of RGO/GCE. More precisely, the oxidation peak current of bare GCE was 349.9 μA (a), RGO/GCE was 309.6 μA (b), and RGO/Fe_3O_4/GCE was 253.8 μA (c). And the peak-to- peak separation (∆Ep) at bare GCE, RGO/GCE and RGO/Fe_3O_4/GCE was 93 mV, 149 mV, 219 mV, respectively. The oxidation peak current decreased obviously and the ∆Ep increased correspondingly, indicating the presence of Fe_3O_4/RGO can slow the electron transfer. The reason why the redox peaks current decreased after being modified lies in the fact that RGO has many hydroxyl and epoxy groups, which can hinder the diffusion of ions and the transfer of electrons to the GCE surface [37, 38]. In order to examine electrochemical behavior and the electron transfer resistance changes of the electrode surface after being modified, the EIS was performed and was shown in Fig. 2.B. Generally, the impedance spectra can be considered to consist of a semicircle portion and a linear portion, and the semicircle portion represents the electron-transfer

resistance (R_{et}) under electro-chemical polarization control at higher frequency range while the linear portion represents the Warburg impedance under concentration polarization control at lower frequency range [29, 39, 40]. The inset in Fig. 2.B is an equivalent circuit of the RGO/Fe_3O_4 electrochemical impedance measurement system, where R_s is the electrolyte resistance which lead to the semicircle beginning at the nonzero intercept of Z', R_{et} is the electron-transfer resistance, Z_w is the Warburg resistance [41]. Fig. 2.B shows that the electron transfer resistance (R_{et}) of bare GCE (a), RGO/GCE (b) and RGO/Fe_3O_4NPs/GCE (c) was about 17 Ω, 30 Ω, 45 Ω, respectively. The result also indicates that the presence of RGO/Fe_3O_4NPs on the surface of bare GCE can slow electron transfer. And these results are in according with CV data in Fig. 2.A.

3.3. Optimization of Scan Rate for Detection of 4-NP

CVs of RGO/Fe_3O_4NPs/GCE in 0.067 M PBS (pH=6.0) with 100 μM 4-NP at different scan rate ranging from 30 to 150 mV s^{-1} are showed in Fig. 3. The oxidation/reduction peak current which increased with the increase of scan rate was clearly observed at the potential of about 0.2 V. The inset in Fig. 3. shows that the oxidation peak current and the square root of scan rate have a linear relationship. The calibration equation can be expressed as I (μA)= 2.13 C $((mV\ s^{-1})^{1/2})$ - 4.47 with the correlation coefficient is 0.995, where C stands for the square root of scan rate. It suggests that the electrode reaction of 4-NP is under diffusion process control. These results also reveal the excellent adsorption properties facilitated by high sheets space and large surface area after compunding RGO with Fe_3O_4NPs [2]. Since the higher scan rate can lead to transient state while the lower scan rate can lead to steady state, so the scan rate of 100 mV s^{-1} was chosen as the scan rate for detection of 4-NP.

3.4. Detection of 4-NP at RGO/Fe_3O_4NPs/GCE

4-NP was detected by DPV and SWV methods in 0.067 M PBS (pH=6.0) on the RGO/Fe_3O_4NPs/GCE. Fig. 4.A shows the DPV curves of different concentration of 4-NP on the RGO/Fe_3O_4NPs modified GCE over the concentration range of 0.2-100 μM. And it can be clearly observed that the potential of peak current for electrochemical detection is at about 0.154V. Fig. 4.B and the inset in Fig. 4.B show the linear relationship between the peak currents and the concentrations from 0.2 μM to 10 μM and 20 μM to 100 μM. And the linear equations respectively are I (μA) = 0.1846C (μM) + 6.1511 (R=0.9983), and I (μA)=0.1071C (μM)+7.6073(R=0.9997), where C stands for the concentration of 4-NP. The limit of detection (LOD) and the limit of quantification (LOQ) were calculated using the following equations: LOD=$3S_B$/b, LOQ=$10S_B$/b, where S_B is the standard deviation of the y-intercepts and b is the slope of the calibration curve [30]. So the LOD and LOQ are 0.26μM, 0.86 μM respectively.

Fig. 5.A shows the SWV curves of different concentration of 4-NP on the RGO/Fe_3O_4NPs/GCE over the concentration range of 0.2-10 μM. And the peak for electrochemical determination of 4-NP can be clearly observed at about 0.152 V. Fig. 5.B shows the linear relationship between the peak currents and the concentrations from 0.2 μM to 10 μM. The peak current and the

concentration of 4-NP showed a linear relationship with the equation I (μA) = 0.295C (μM) + 11.36 (R=0.9946), where C stands for the concentration of 4-NP. The LOD and LOQ reached 12 nM, 40 nM respectively.

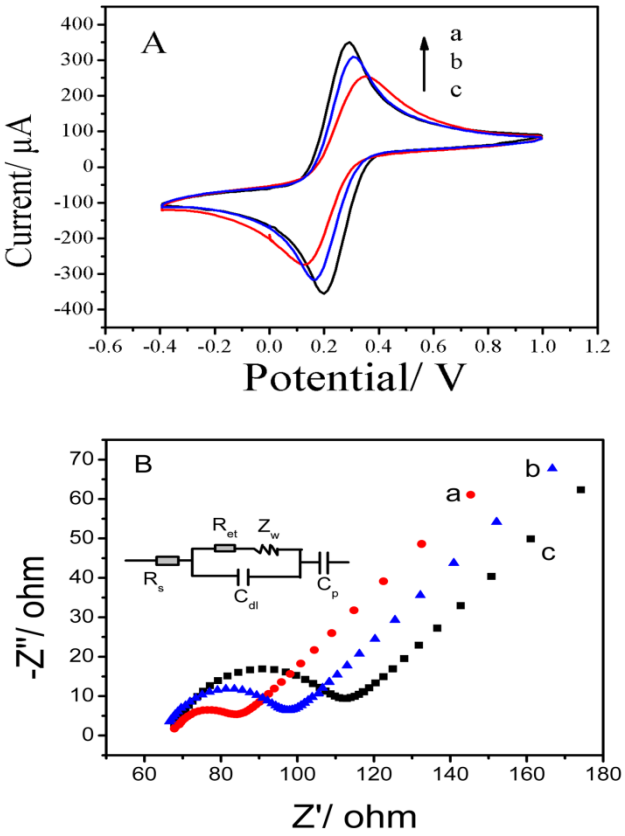

Figure 2. (A) CVs of (a) bare GCE, (b) RGO/GCE, and (c) RGO/Fe_3O_4NPs/GCE in the 0.1M KCl solution of 0.01M $[Fe(CN)_6]^{3-/4-}$. Scan rate was 100mV s^{-1}. (B) Nyquist plots of (a) bare GCE, (b) RGO/GCE, and (c) RGO/Fe_3O_4NPs/GCE in the 0.1M KCl solution of 0.01M $[Fe(CN)_6]^{3-/4-}$.

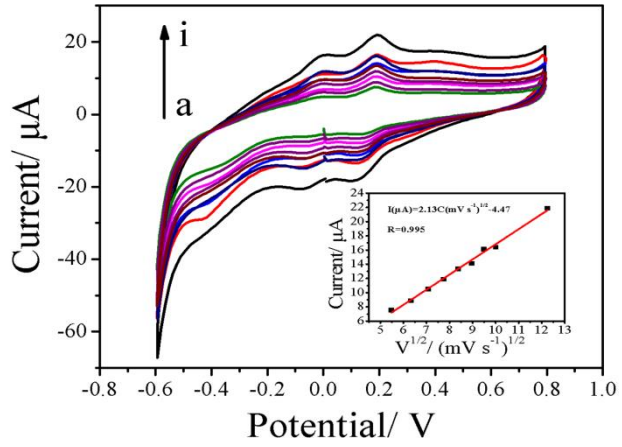

Figure 3. CVs of RGO/Fe_3O_4NPs/GCE with 100 μM 4-NP in 0.067 M PBS (pH=6.0) at different scan rate ranging from 30 to 150 mV s^{-1}. $V^{1/2}$ ((mV s^{-1})$^{1/2}$) : (a)30;(b)40;(c)50;(d)60;(e)70;(f)80;(g)90;(h)100;(i)150. Inset figure shows plots of peak currents vs. square root of scan rates.

A comparison of analytical parameters of the reported different electrochemical sensors and the present sensor for the detection of 4-NP is summarized in Table 1. Clearly, the RGO/Fe_3O_4NPs/GCE sensor has a high correlation coefficient, satisfactory linear range, lowest detection limit due to the synergistic effect of Fe_3O_4NPs and RGO. The excellent performance is attribute to Fe_3O_4NPs acted as nanoscale spacers between the two adjacent RGO sheets and effectively prevented the RGO sheets from re-stacking together [42, 43]. The results clearly show that the RGO/Fe_3O_4NPs/GCE had excellent capacity for the determination of 4-NP. So it is feasible for the electrochemical sensors based on RGO/Fe_3O_4NPs/GCE to detect the trace of 4-NP in water.

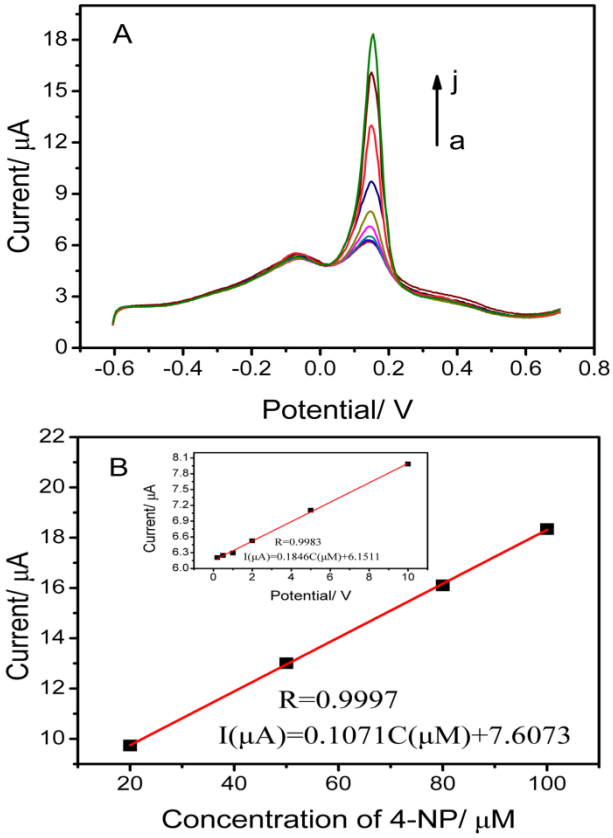

Figure 4. (A) DPV response of different concentration of 4-NP: (a)0.2;(b)0.5;(c)1;(d)2;(e)5;(f)10;(g)20;(h)50;(i)80;(j)100 μM on RGO/Fe_3O_4/GCE in 0.067 M PBS (pH=6.0). Amplitude: 20 mV; Increment: 5 mA; Pluse period : 200 ms; Pluse width: 100 ms; Scan rate: 100 mV s^{-1}. (B) and the inset shows corresponding calibration plot of the DPV curves of 0.2-10μM and 20-100μM respectively.

3.5. Recovery and stability of RGO/Fe_3O_4NPs/GCE

For practice, a recovery experiment was performed to examine the potential applications of the RGO/Fe_3O_4NPs/GCE. So RGO/Fe_3O_4NPs/GCE sensor was adopted to detect the different concentration of 4-NP in the tap water. Before detection, the pH of the tap water need to be adjusted to 6.0 with Na_2HPO_4 and NaH_2PO_4. And before 4-NP was added, there was no response current of 4-NP.

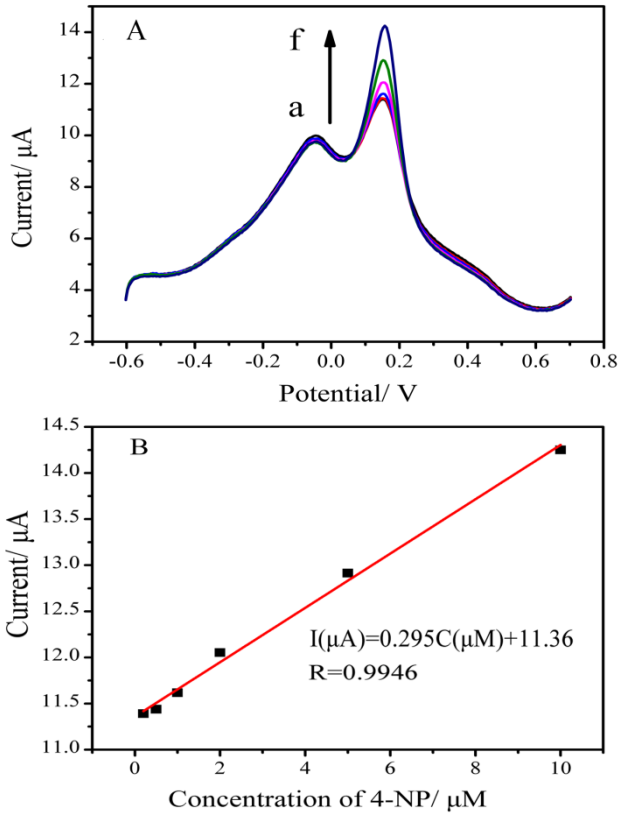

Figure 5. (A)SWV response of different concentration of 4-NP: (a)0.2;(b)0.5;(c)1;(d)2;(e)5;(f)10μM on RGO/Fe_3O_4/GCE in 0.067 M PBS (PH=6.0). Amplitude: 20mV; Increment: 5 mA; Pluse period: 200 ms; Scan rate: 100 mV s^{-1}. (B)Corresponding calibration plot of the SWV curves of 0.2-10 μM.

Table 1. Comparison of different sensors for detection 4-NP.

Modified electrodes	Linear range (μM)	Stability (days)	Detection limit (μM)	Correlation Coefficient	Recovery	References
GO/GCE	0.1-120	83%(30)	0.02	0.9975	99-102.3	44
RGO/AuNPs/GCE	0.05-2	98%(14)	0.01	0.9981	98-104	45
	4-100	90%(35)		0.9975		
AC[a] /GCE	1-500	88%(25)	0.16	0.9863	----	2
MnO_2/RGO	1-100	94%(14)	0.017	0.9995	99.2-101.1	41
HN[b]/GCE	1-300	82%(30)	0.6	0.9996	96-104	46
DTD[c]/AgNPs/CPE[d]	1-100	----	0.25	----	99-101	47
ZnO/F/GCE[e]	0.035-1.4	94%(7)	0.008	0.9988	97-106	48
	2.1-6.3			0.9977		
pCu/GPE[f]	50-850	----	1.91	0.9997		49
RGO/Fe_3O_4NPs/GCE	0.2-10	91%(20)	0.26	0.9983	98-101.7	This work
	20-100			0.9997		

[a] AC: activated carbon. [b] HN: hydroxyapatite nanopowder. [c] DTD: synthetic ligand: 6,7,9,10,17,18,19,20,21,22 – decahydrodibenzo [h,r] [1,4,7,11,15] trioxadiazacyclonanodecine – 16,23dione. [d] CP: carbon paste electrode. [e] ZnO/F/GCE: ZnO film - coated GCE. [f] pCu/GPE: porous Cu-modified graphite pencil electrode.

Table 2. Detection of 4-NP from the water sample.

Add (μM)	DPV method		SWV method	
	Detection (μM)	Recovery (%)	Detection (μM)	Recovery (%)
0.5	0.49	98	0.507	101.4
2	1.987	99.3	1.983	99.1
5	5.044	100.9	5.062	101.2
20	20.346	101.7	----	----
50	49.261	98.5	----	----

Then 4-NP was added with different concentrations to the water sample, the results of different concentrations detected by both DPV and SWV methods are showed in Table 2. And the recoveries were found with the range from 98 to 101.7, indicating this sensor can be used in practice.

In order to determine storage stability of the RGO/Fe_3O_4NPs, its 4-NP detection performance was monitored every three or four days for 20 days. Fig. 6 shows the relationship between the peak current and different days. During 20 days storage period, the RGO/Fe_3O_4NPs electrode retained 91% of initial response current which revealing good storage stability.

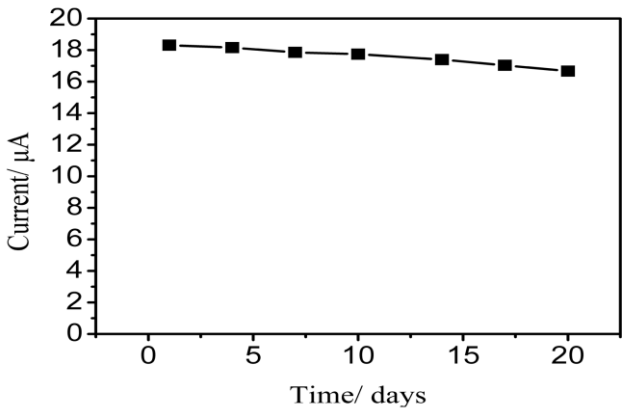

Figure 6. Peak current of different storage days of 4-NP on RGO/Fe_3O_4/GCE in 0.067 M PBS (PH=6.0) by DPV response. Amplitude: 20mV; Increment: 5 mA; Pluse period : 200 ms; Pluse width: 100 ms; Scan rate: 100 mV s^{-1}.

4. CONCLUSIONS

In this study, an excellent RGO/Fe_3O_4NPs modified electrode was adopted to detect 4-NP. The surface morphology of the prepared RGO/Fe_3O_4NPs was confirmed via SEM images, which showed that the Fe_3O_4NPs were successfully adhered to the surface and the inside of RGO and they are well dispersed with little coagulation. And the electrochemical behaviors of RGO/Fe_3O_4NPs/GCE was investigated with the DPV method and SWV method, and the result was satisfactory because of the

high correlation coefficient, excellent linear range, favorable stability and good recovery. And the LOD and LOQ reached 0.26 μM, 0.86 μM respectively. So this sensor maybe a good choice in practical applications.

ACKNOWLEDGEMENTS
The authors are grateful for the support by the National Natural Science Foundation of China (No.51622507, 61471255, 61474079, 61501316, 51505324), Doctoral Fund of MOE of China (No.20131402110013), 863 project (2015AA042601).

References

1. C. Nistor, A. Oubiña, M. P. Marco, D. Barceló and J. Emnéus, *Anal. Chim. Acta,* 426 (2001) 185.
2. R. Madhu, C. Karuppiah, S. M. Chen, P. Veerakumar and S.-B. Liu, *Anal. Methods,* 6 (2014) 5274.
3. Z. Dong, X. Le, C. Dong, W. Zhang, X. Li and J. Ma, *Appl. Catal., B: Environ.,* 162 (2015) 372.
4. S. R. Rui, A. M. T. Silva, H. T. Gomes and J. L. Faria, *U. Porto J. Eng.,* 1 (2015) 50.
5. J. Karaová, J. Barek and K. Schwarzová-Pecková, *Anal. Lett.,* 49 (2016) 66.
6. C. Borras, T. Laredo, J. Mostany and B. Scharifker, *Electrochim. Acta,* 49 (2004) 641.
7. T. Hao, X. Wei, Y. Nie, Y. Xu, Y. Yan and Z. Zhou, *Microchim. Acta,* 183 (2016) 2197.
8. X. Guo, Z. Wang and S. Zhou, *Talanta,* 64 (2004) 135.
9. H. R. Sobhi, A. Esrafili, H. Farahani, M. Gholami and M. M. Baneshi, *Environ. Monit. Assess.,* 185 (2013) 9055.
10. J. Cacho, N. Campillo, P. Viñas and M. Hernández-Córdoba, *J. Chromatogr. A,* 1241 (2012) 21.
11. L. H. Zhang, W. C. Li, D. Yan, H. Wang and A. H. Lu, *Nanoscale,* 8 (2016) 13695.
12. Z. Wu, B. Yan, D. Liang, M. Guo and X. Zhang, *J. Chin. Inst. Food.Sci.Tech.,* 15 (2015) 166.
13. T. Widaningrum, E. Widyastuti, F. W. Pratiwi, I. F. F. Ai, P. Rijiravanich, M. Somasundrum and W. Surareungchai, *Talanta,* 167 (2017) 14.
14. J. He, J. Sunarso, Y. Zhu, Y. Zhong, J. Miao, W. Zhou and Z. Shao, *Sens. Actuators B: Chem.,* 244 (2017) 482.
15. Y. Guo, S. Guo, J. Ren, Y. Zhai, S. Dong and E. Wang, *Acs Nano,* 4 (2010) 4001.
16. S. Sattayasamitsathit, A. M. O'Mahony, X. Xiao, S. M. Brozik, C. M. Washburn, D. R. Wheeler, J. Cha, D. B. Burckel, R. Polsky and J. Wang, *Electrochem. Commun.,* 13 (2011) 856.
17. K. S. Min, B. Lee, H. K. Shi, J. A. Lee, G. M. Spinks, S. Gambhir, G. G. Wallace, M. E. Kozlov, R. H. Baughman and S. J. Kim, *Nat. Commun.,* 3 (2012) 19596.
18. L. S. Walker, V. R. Marotto, M. A. Rafiee, N. Koratkar and E. L. Corral, *Acs Nano,* 5 (2011) 3182.
19. J. Xiao, D. Mei, X. Li, W. Xu, D. Wang, G. L. Graff, W. D. Bennett, Z. Nie, L. V. Saraf and I. A. Aksay, *Nano lett.,* 11 (2011) 5071.
20. J. Wang, M. Liang, Y. Fang, T. Qiu, J. Zhang and L. Zhi, *Adv. Mater.,* 24 (2012) 2874.
21. A. Yu, I. Roes, A. Davies and Z. Chen, *Appl. Phys. Lett.,* 96 (2010) 253105.
22. H. J. Yoon, D. H. Jun, J. H. Yang, Z. Zhou, S. S. Yang and M. C. Cheng, *Sens. Actuators B: Chem.,* 157 (2011) 310.
23. W. M. Zhang, X. L. Wu, J. S. Hu, Y. G. Guo and L. J. Wan, *Adv. Funct. Mater.,* 18 (2008) 3941.
24. S. Ito, K. Nakaoka, M. Kawamura, K. Ui, K. Fujimoto and N. Koura, *J. Power Sources,* 146 (2005) 319.
25. P. L.Taberna, S. Mitra, P. Poizot, P. Simon and J. M. Tarascon, *Nature mater.,* 5 (2006) 567.
26. G. Zhou, D. W. Wang, F. Li, L. Zhang, N. Li, Z. S. Wu, L. Wen, G. Q. Lu and H. M. Cheng, *Chem. Mater.,* 22 (2010) 5306.
27. M. B. Gawande, P. S. Branco and R. S. Varma, *Chem. Soc. Rev.,* 42 (2013) 3371.

28. J. E. Lee, N. Lee, H. Kim, J. Kim, S. H. Choi, J. H. Kim, T. Kim, I. C. Song, S. P. Park and W. K. Moon, *J. Am. Chem. Soc.*, 132 (2009) 552.
29. W. J. Li, X. Z. Yao, Z. Guo, J. H. Liu and X. J. Huang, *J. Electroanal. Chem.*, 749 (2015) 75.
30. M. R. Mahmoudian, Y. Alias, W. J. Basirun, M. W. Pei, M. Sookhakian and F. Jamali-Sheini, *Electrochim. Acta*, 169 (2015) 126.
31. F. Ning, H. Peng, J. Li, L. Chen and H. Xiong, *J. Agric. Food Chem.*, 62 (2014) 7436.
32. N. Nazari, M. Masrournia, H. Z. Es and M. Bozorgmehr, *J. Sep. Sci.*, 39 (2016) 3046.
33. G. J. Rani, K. J. Babu, G. G. Kumar and M. A. J. Rajan, *J. Alloys Compd.*, 688 (2016) 500.
34. C. H. Hong, M. W. Kim, W. L. Zhang, I. J. Moon and H. J. Choi, *J. Colloid Interface Sci.*, 481 (2016) 194.
35. Y. Qin, M. Long, B. Tan and B. Zhou, *Nano-Micro Lett.*, 6 (2014) 125.
36. B. Yang, Z. Tian, L. Zhang, Y. Guo and S. Yan, *J. Water Process Eng.*, 5 (2015) 101.
37. H. He, J. Klinowski, M. Forster and A. Lerf, *Chem. Phys. Lett.*, 287 (1998) 53.
38. A. Lerf, H. He, M. Forster and J. Klinowski, *J. Phys. Chem. B*, 102 (1998) 4477.
39. Y. Wei, R. Yang, Y. X. Zhang, L. Wang, J. H. Liu and X. J. Huang, *Chem. Commun.*, 47 (2011) 11062.
40. Y. Wei, L. T. Kong, R. Yang, L. Wang, J. H. Liu and X. J. Huang, *Chem. Commun.*, 47 (2011) 5340.
41. Y. Haldorai, K. Giribabu, S. K. Hwang, C. H. Kwak, S. H. Yun and Y. K. Han, *Electrochim. Acta*, 222 (2016) 717.
42. X. Dong, L. Li, C. Zhao, H. K. Liu and Z. Guo, *J. Mater. Chem. A*, 2 (2014) 9844.
43. K. Zhang, W. Zhao, J. T. Lee, G. Jang, X. Shi and J. H. A. Park, *J. Mater. Chem. A*, 2 (2014) 9636.
44. J. Li, D. Kuang, Y. Feng, F. Zhang, Z. Xu and M. Liu, *J. Hazard. Mater.*, 201–202 (2012) 250.
45. Y. Tang, R. Huang, C. Liu, S. Yang, Z. Lu and S. Luo, *Anal. Methods*, 5 (2013) 5508.
46. H. Yin, Y. Zhou, S. Ai, X. Liu, L. Zhu and L. Lu, *Microchim. Acta*, 169 (2010) 87.
47. G. Rounaghi and H. Azizi-toupkanloo, *Mater. Sci. Eng., C*, 32 (2012) 172.
48. R. Bashami, A. Hameed, M. Aslam, I. M. I. Ismail and M. T. Somroo, *Anal. Methods*, 7 (2015) 1794.
49. A. Kawde and M. A. Aziz, *Electroanalysis*, 26 (2014) 2484.